

- (22) Hollo, J.; Laszlo, E.; Hoschke, A. *Stärke* 1964, 16, 243-246.  
 (23) Kamogawa, A.; Fukui, T.; Nikuni, Z. *J. Biochem. (Tokyo)* 1968, 63, 361-369.  
 (24) Husemann, E.; Pfannemüller, B. *Makromol. Chem.* 1961, 49, 214-237.  
 (25) Pfannemüller, B. *Stärke* 1968, 20, 351-362.  
 (26) Gidley, M. J.; Bulpin, P. V. *Carbohydr. Res.* 1987, 161, 291-300.  
 (27) Praznik, W.; Ebermann, R. *Stärke* 1979, 31, 288-293.  
 (28) Everett, W. W.; Foster, J. F. *J. Am. Chem. Soc.* 1959, 81, 3464-3469.  
 (29) Cowie, J. M. G. *Makromol. Chem.* 1961, 42, 230-247.  
 (30) Burchard, W. *Makromol. Chem.* 1963, 64, 110-125.  
 (31) Banks, W.; Greenwood, C. T. *Carbohydr. Res.* 1968, 7, 414-420.  
 (32) Gidley, M. J. *Carbohydr. Res.* 1985, 139, 85-93.  
 (33) Rees, D. A.; Morris, E. R.; Thom, D.; Madden, J. K. *The Polysaccharides*; Academic: New York, 1982; Vol. 1, pp 195-290.  
 (34) Jane, J.-L.; Robyt, J. F. *Carbohydr. Res.* 1984, 132, 105-118.  
 (35) Eberstein, K.; Höpcke, R.; Konieczny-Janda, G.; Stute, R. *Stärke* 1980, 32, 397-404.  
 (36) Stute, R.; Konieczny-Janda, G. *Stärke* 1983, 35, 340-347.

## Rheological Studies of Aqueous Amylose Gels: The Effect of Chain Length and Concentration on Gel Modulus

Allan H. Clark, Michael J. Gidley,\* Robert K. Richardson, and Simon B. Ross-Murphy

Unilever Research Laboratory, Colworth House, Sharnbrook, Bedford, MK44 1LQ, U.K.  
 Received January 20, 1988; Revised Manuscript Received June 2, 1988

**ABSTRACT:** Aqueous amylose gels have been studied kinetically and at pseudoequilibrium as a function of polymer concentration and chain length. Pseudoequilibrium gel moduli ( $G'$ ) for a range of amylose chain lengths (produced by enzymatic synthesis) show the same concentration dependences as other gelling biopolymers and have been analyzed by the method of Clark and Ross-Murphy (*Br. Polym. J.* 1985, 17, 164-168). This treatment is shown to lead to the accurate prediction of critical gelling concentrations and suggests that the cross-linking functionality of individual amylose chains is  $\sim DP/100$  ( $DP$  = degree of polymerization). For a fixed concentration, shorter chain amylose systems are found to develop turbidity more rapidly and to attain higher final values, suggesting that decreasing amylose chain length results in more heterogeneous gel structures. The relative rates of turbidity and modulus increase for amylose gels are found to be dependent on chain length: for short chains ( $DP < 300$ ) turbidity precedes gelation, whereas for longer chains ( $DP < 1100$ ) gelation occurs before significant increase in turbidity.

### Introduction

Amylose is a polysaccharide component of starch and, in nature, is a polydisperse  $\alpha$ -(1 $\rightarrow$ 4) glucan which can be linear or lightly branched<sup>1</sup> (through additional  $\alpha$ -(1 $\rightarrow$ 6) linkages). Fractionation of starch<sup>1,2</sup> yields amylose preparations that are inherently unstable in aqueous solution at room temperature.<sup>2,3</sup> Amylose precipitates from dilute aqueous solution, whereas gels are formed from more concentrated systems.<sup>2,3</sup> It is thought that gelation of the amylose component is important in starch gelation, at least during the initial stages.<sup>4</sup> Recently, the mechanisms involved in amylose gelation have been addressed,<sup>5</sup> and some of the factors which affect the gelation process have been investigated.<sup>6</sup>

Two of the most important variables in amylose gelation are polymer concentration and chain length.<sup>3,6,7</sup> In the preceding paper in this issue,<sup>7</sup> nearly monodisperse enzymically synthesized amyloses were used to characterize the phase change behavior and polymer aggregation kinetics of aqueous amylose systems. It was found that precipitation (and not gelation) occurred for chain lengths of  $DP$  (degree of polymerization)  $< 110$ , whereas gelation occurred for amyloses of  $DP > 250$  at concentrations of  $> 1.0\%$ . In this report, we describe rheological studies of aqueous gels of enzymically synthesized amyloses with particular regard to the effect of polymer chain length and concentration. Although enzymically synthesized samples have provided much insight into chain length effects in dilute amylose solutions,<sup>8,9</sup> we are not aware of any studies of amylose gelation using such essentially monodisperse materials.

### Methods

**Synthesis and Characterization of Amylose Samples.** The synthesis of amyloses using maltoheptaose as a primer, glucose

1-phosphate as monomer, and the enzyme phosphorylase as catalyst was carried out as described in the preceding paper.<sup>7</sup> Gel permeation chromatography was used to show that synthesized amyloses had a narrow molecular weight distribution<sup>7</sup> ( $M_w/M_n < 1.15$  and typically  $< 1.10$ ), and chain lengths were determined from intrinsic viscosity measurements in dimethyl sulfoxide and from analysis of polymerization solutions for inorganic phosphate.<sup>7</sup>

**Preparation of Aqueous Amylose Gels.** Gels were prepared by cooling clear aqueous solutions of amylose. Solutions were obtained by heating appropriate mixtures of amylose and deionized water in sealed tubes at 160 °C for 10-15 min<sup>7</sup>. After cooling to 70-80 °C, the tubes were opened, and the solutions were immediately transferred into (as appropriate) a mechanical spectrometer, a driven torsion pendulum, or a spectrophotometer cell and subjected to controlled cooling regimes as detailed below.

**Rheological and Turbidimetric Measurements.** The development of gel structure was monitored by small deformation mechanical measurements obtained by using a driven torsion pendulum<sup>10</sup> or a Rheometrics mechanical spectrometer (RMS-605).<sup>11</sup> Hot aqueous amylose solutions were introduced into the sample cell of the torsion pendulum or between parallel plates in the mechanical spectrometer, a thin layer of light silicone oil was added to prevent evaporative loss, and the samples were cooled from 60 to 25 °C at a rate of  $\sim 1$  °C/min and held at 25 °C. For analysis of amylose concentration dependence, modulus values were recorded after 200 min at 10 rad s<sup>-1</sup> and 2% strain. Sample temperatures were continuously monitored to enable turbidity measurements to be carried out under identical cooling regimes. Turbidity data were obtained for amyloses having a range of chain lengths and concentrations under temperature/time profiles directly comparable with those of rheological measurements, using a Beckman DU7 spectrophotometer at 700 nm and with a pathlength of 1 cm.

### Results

Figure 1 shows the change in shear modulus ( $G'$ ) at 10 rad s<sup>-1</sup> which takes place on cooling aqueous solutions of amylose having a  $DP_n$  of  $\sim 1100$ . These traces follow the

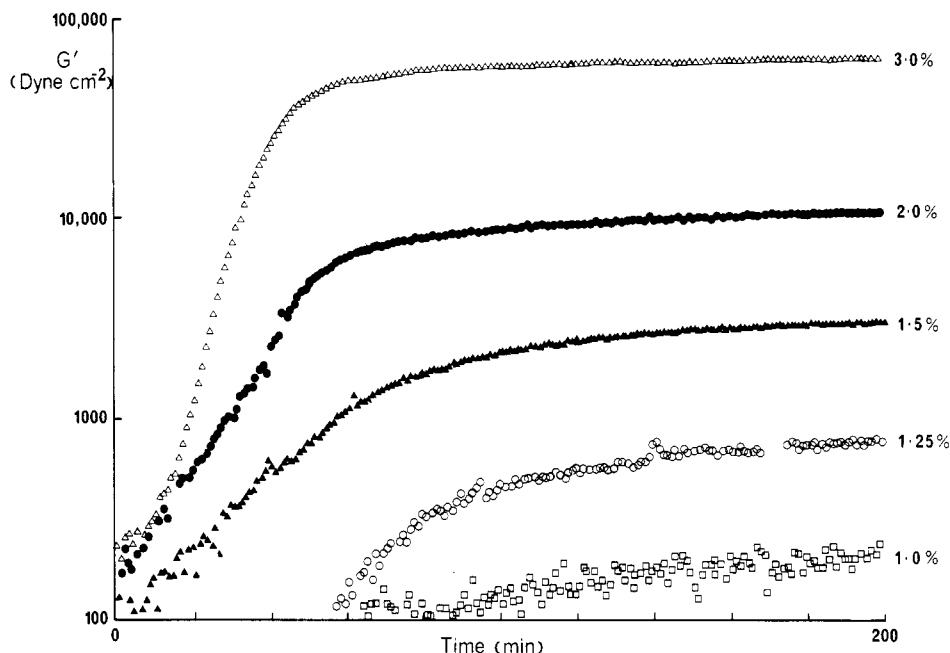


**Figure 1.** Storage modulus ( $G'$ ) vs time for various concentrations of amylose, DP = 1100. Data were obtained every 60 s on a Rheometrics mechanical spectrometer at  $10 \text{ rad s}^{-1}$  and 0.32% strain. The point to point scatter provides an estimate of the experimental uncertainty.

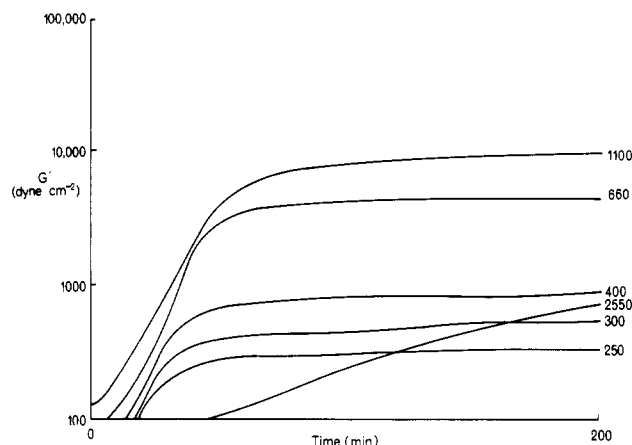


**Figure 2.** Storage modulus vs time for 2% aqueous amyloses having chain lengths (DP) as shown and determined as for Figure 1. Individual data points showed similar scatter to those in Figure 1 and are omitted for clarity.

expected<sup>12</sup> behavior with an initial rapid rise in modulus followed by a much slower increase on attainment of the pseudoplateau region. For all chain lengths studied (DP = 250, 300, 400, 660, 1110, 2550, and 2800) the initial rise in modulus is faster, and the pseudoplateau region is reached at shorter times with increasing amylose concentration.

Figure 2 shows a comparison of  $G'$ /time profiles for cooled 2% aqueous solutions of amylose having different chain lengths. For amyloses of DP = 250–1100, qualitatively similar profiles are observed with the pseudoplateau region being attained earlier and the subsequent modulus increase being slightly less for shorter chain lengths. Amyloses of DP = 2550 and 2800 show very similar  $G'$ /time profiles that are different from those of amyloses of lower DP (250–1100). A pseudoplateau region characteristic of gels formed from amyloses of DP = 250–1100 (Figures 2 and 3) is not observed, at least in the initial 2 weeks, for DP = 2550 (or 2800), which instead shows a gradual rise in shear modulus (Figure 3). Whereas for a given concentration  $G'$  is greater for increasing chain lengths (up to 1100) at all stages of the cool and cure process (Figure 2), the 2% DP = 2550 system only attains

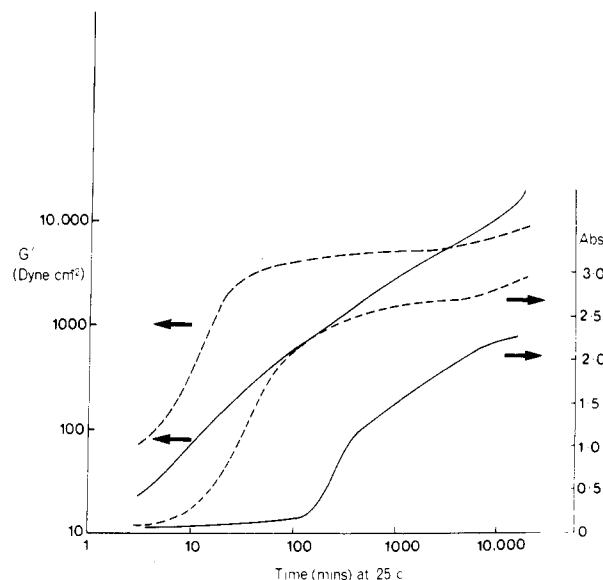


**Figure 3.** Comparison of  $G'$  (determined by using a driven torsion pendulum and shown on the left-hand axis) and turbidity development (right-hand axis) for 2% aqueous amyloses of DP = 2550 (solid lines) and DP = 660 (dashed line).

the same modulus as the 2% DP = 660 system after 58 h (Figure 3).

Turbidity data were also obtained under identical temperature/time regimes as rheological measurements: typical results are shown in Figures 3 and 4. For all amylose chain lengths, increases in turbidity are observed on cooling hot aqueous solutions<sup>7</sup> (e.g., Figures 3 and 4). However, depending on the amylose chain length, turbidity increases either precede or lag behind increases in  $G'$ . Thus, for amylose of DP = 250, turbidity increases (Figure 4) occur before noticeable modulus development (Figure 2), whereas for amyloses of DP = 1100 (Figures 2 and 4) and particularly DP = 2550 (Figure 3), increases in turbidity lag behind increases in  $G'$ . At intermediate chain lengths of 400 and 660 (Figures 2 and 4),  $G'$  and turbidity show similar time/temperature dependences.

To characterize amylose gels formed in the mechanical spectrometer, the effects of frequency and strain on shear

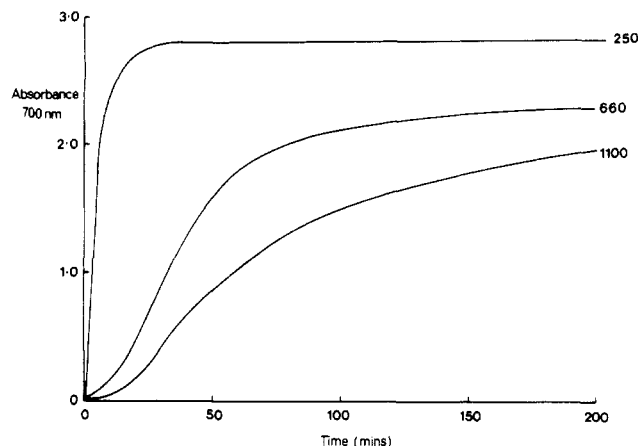


**Figure 4.** Turbidity vs time over temperature profiles identical with Figures 1 and 2 for 2% aqueous amyloses having chain lengths (DP) as shown.

modulus were investigated for each sample following the 200-min cool and cure period (Figures 1 and 2).  $G'$  is found to be essentially independent of frequency in the range  $10^{-2}$ – $10^2$  rad s $^{-1}$  and strain in the range 1–5%. For all amylose gels studied, values of  $G''$  were found to be less than 100 dyn cm $^{-2}$ , i.e., for the observed values of  $G^*$  below the reliable phase angle resolution limit of the mechanical spectrometer in the configuration used.

Pseudoequilibrium values of  $G'$  were measured for amyloses of DP < 1100 after ~210 mins at 10 rad/s by extrapolating to zero strain from a  $G'$  vs strain plot. These values were used in subsequent analyses of the effect of concentration and chain length on amylose gel modulus.

## Discussion

**Effects of Chain Length and Concentration on the Kinetics of Gel Modulus Evolution.** The general features of the evolution of modulus with time for gels formed from amyloses of DP = 250–1100 (Figures 1 and 2), i.e., an initial rapid rise followed by slower increases at longer times (and  $G' > G''$ ), are typical of aqueous biopolymer gels.<sup>12</sup> The initial rise in modulus follows the establishment of a three-dimensional network structure and involves the conversion of increasing amounts of chains in the sol fraction into the gel; the subsequent slower rise in modulus would then be caused by further cross-linking paralleled by annealing processes such as rearrangement of cross-links and lateral chain aggregation resulting in a net decrease in the length of elastically active chains. The transition from the stage of rapidly increasing modulus to the pseudoplateau stage presumably occurs when most (or virtually all) of the sol fraction has been converted into the gel phase. The slightly greater increase in modulus in the pseudoplateau region (Figure 2) for amylose gels formed from longer chains (up to DP = 1100) suggests that the annealing processes become more prevalent for longer chain lengths. Such an apparent three-stage process (i.e., lag, rapid increase, and terminal stages) is to be expected from the time dependence of cross-linking, and of modulus increase, and has been seen quite generally in other cross-linking systems.<sup>12</sup>

For amyloses of DP > 200 it has been found<sup>7,9</sup> that aggregation in aqueous solution is slower for increasing chain lengths. The results depicted in Figure 2 show that similar chain length effects are observed in the development of gel moduli; i.e., the  $G'$  pseudoplateau region is reached sooner for shorter chain lengths at 2% concentration. This chain length effect is more pronounced if systems with similar pseudoequilibrium moduli are com-

pared, e.g., 1.25% DP = 1100 (Figure 1) and 2.0% DP = 300 (Figure 2). These systems have similar moduli after 200 min, but the initial rate of modulus increase is faster, and the time taken to reach the pseudoplateau region is less with decreasing amylose chain length.

The relative  $G'$  vs time behavior of amyloses of DP = 1100 and 2550 follow the same trend, but the significant differences in the  $G'$ /time profiles for DP = 2550 amylose (Figure 3) compared with amyloses of DP = 1100 and less (Figures 2 and 3) suggest that there may be a different rate-limiting effect on modulus increase for long chains. A factor which may be important in the slow development of modulus for DP = 2550 amylose could be that, for such long chains, relatively few cross-links are required before aggregate diffusion becomes significantly retarded, thereby slowing down subsequent cross-linking and modulus increase. The fact that sol fraction diffusion would in any case be slower for longer chains may also be important.

A practical consequence of the very slow development of  $G'$  for amyloses of DP = 2500–3000 is that measurements of shear modulus for different chain lengths at a fixed cure time may give apparently surprising results. Thus, for a cure time of <58 h, a 2% gel of DP = 660 amylose has a higher  $G'$  than a 2% DP = 2550 gel (Figure 3), in contradiction to the expected result of increased gel modulus with increasing chain length (see later). In a recent study,<sup>6</sup> Ellis and Ring presented shear modulus data which suggested that increased amylose chain length resulted in decreased shear moduli for 3.5% gels. However, as the (polydisperse) fractions studied had average DP<sub>w</sub> values of 3000–7000, the moduli obtained may have been intermediate values on a steadily increasing  $G'$ /time profile (e.g., Figure 3) with longer chains showing slower modulus development and lower moduli at a fixed time than gels formed from longer chains. At the cure times used by Ellis and Ring<sup>6</sup> (24–48 h), for example, the modulus of a 2% DP = 660 amylose gel is greater than that of a 2% DP = 2550 gel (Figure 3), although the final (infinite time) modulus is undoubtedly greater for the longer chain length. Alternatively, the discrepancy between the results of Ellis and Ring<sup>6</sup> (who found shear modulus to decrease with increasing chain length) and the present data may be due to the different sample preparation conditions used. Ellis and Ring<sup>6</sup> prepared gels by quenching hot (368 K) aqueous solutions to 293 K whereas we have used a slow controlled-cooling regime. It may be possible that quenching conditions limit the long-time annealing processes which we have observed (Figure 4) and thereby lead to a kinetically trapped gel structure further from pseudoequilibrium than gels formed under slow cooling conditions. By analogy with the results shown in Figure 4, this may lead to an apparent inverse relationship between gel modulus and amylose chain length.

**Comparison of Modulus and Turbidity Data for Amylose Gels as a Function of Chain Length.** On cooling hot aqueous solutions of amylose, opacity develops for all chain lengths.<sup>7</sup> Initial rates of turbidity development show a strong dependence on chain length<sup>7</sup> with a maximum at DP ~ 100. The rate of turbidity increase is less, and the long-time (10 000 min) absorbance value is lower with increasing chain length above DP = 100 (Figures 3 and 4 and ref 7). These data suggest that, at any fixed cure time, gel networks formed from longer amylose chains are more homogeneous.

Figures 2–4 may be used to compare modulus and turbidity data for amyloses of various chain lengths having identical thermal histories. For a chain length of 250 (Figures 2 and 4), a 2% aqueous system shows substantial

turbidity ( $\sim 2.3$  absorbance units) before detectable modulus is apparent ( $\sim 10$  min), and a pseudoplateau of turbidity is reached soon after (Figure 4), whereas the modulus increases significantly for  $\sim 60$  min (Figure 2). This comparison suggests that substantial aggregation can occur for this amylose chain length without contributing markedly to the modulus.

At the other extreme of amylose chain length used in this study, however, the situation is very different. For 2% DP = 2550 amylose (Figure 3), there is only a slight rise in turbidity over the first 100 min during which time  $G'$  has risen to  $\sim 10^3$  dyn cm $^{-2}$ . Subsequently, turbidity increases at approximately the same rate as the shear modulus (Figure 3). The observation that turbidity increases lag behind modulus development for DP = 2550 suggests that the network structure formed initially (0–100 min) is not markedly heterogeneous (on a submicron distance scale). The subsequent rise in turbidity shows that the annealing gel becomes progressively more heterogeneous, suggesting significant localized chain aggregation.

For intermediate chain lengths, comparisons of turbidity and modulus development show intermediate behavior (Figures 2–4); i.e., for DP = 300, turbidity precedes significant modulus development; for DP = 400 and 660, turbidity and modulus changes occur over similar time scales; and for DP = 1100, a modulus increase occurs more rapidly than rises in turbidity. Such comparisons suggest that the more heterogeneous (turbid) gels obtained from shorter amyloses reflect increasing participation of rapid<sup>7</sup> aggregation processes (e.g., precipitation), which do not contribute significantly to the gel modulus.

Although all gelling amyloses show turbidity, the variation in the time scales of modulus and absorbance development as a function of chain length suggests that the processes which lead to gelation and turbidity in aqueous amylose systems are not directly related.

**Concentration Dependence of Gel Modulus as a Function of Amylose Chain Length.** Clark and Ross-Murphy have recently discussed<sup>12,13</sup> the relationship between shear modulus (in practice the storage component  $G'$ ) and concentration for protein and polysaccharide gels. Their method, which has subsequently been applied with success to a number of other systems, effectively factorizes the modulus into two terms, one describing the number of elastically effective chains and the second, the contribution per chain to the modulus (which includes local, chain stiffness, effects). The relationship between  $G'$  and  $C$  has as parameters  $M$ , the molecular weight of the network-forming material;  $f$ , the number of sites available for cross-linking per polymer molecule;  $K$ , the equilibrium constant for the making and breaking of cross-links; and  $a$ , the generalized front factor. This last quantity is introduced to replace the classical front factor of unity usually employed in the classical (entropic) theory of rubber elasticity,<sup>14</sup> an elastically active network chain<sup>15,16</sup> in a biopolymer network being allowed to contribute an amount  $akT$  to the shear modulus rather than  $kT$  as in the classical theory. For globular protein gels,<sup>17</sup> and certain gels from polysaccharides,<sup>12,13</sup>  $a$  can be 1 order of magnitude (or more) greater than unity.

The application to amylose modulus-concentration data of the Clark-Ross-Murphy approach<sup>12,13</sup> is particularly worthwhile since  $M$  is known and the samples studied are essentially monodisperse. As in similar analyses of data for other gelling systems, there are difficulties and sources of uncertainty,<sup>18</sup> and these should be briefly pointed out before results are discussed. First, as is true of other polysaccharide gels such as those from agarose,<sup>19</sup> some

**Table I**  
Details of Best Fits to  $G'$  versus Concentration Data for DP = 660 Amylose Gels Obtained by Using the Clark-Ross-Murphy Approach<sup>a</sup>

model functionality $f$	$a$	$K$ , L mol $^{-1}$	$C_0$ , % w/w
3	24.1	$0.653 \times 10^4$	1.09
5	11.1	$0.870 \times 10^3$	1.09
10	6.8	$0.138 \times 10^3$	1.09
20	5.4	$0.290 \times 10^2$	1.08
100	4.3	$0.103 \times 10^1$	1.07
1000	4.1	$0.100 \times 10^{-1}$	1.07

<sup>a</sup> High correlation between  $a$ ,  $K$ , and  $f$  values is evident.  $C_0$  varies only slightly.

**Table II**  
Critical Concentration ( $C_0$ ) Results for DP = 300, 660, 1100, and 2550 Amylose Gels Obtained by Fitting  $G'$  versus Concentration Data

DP	$C_0$ , % w/w	DP	$C_0$ , % w/w
300	1.0	1100	0.8
660	1.1	2550	1.1

<sup>a</sup> To the accuracy quoted, these results are independent of the choice of  $f$ .

cross-links may form essentially irreversibly, whilst the original theoretical approach relied on assumption of an equilibrium between bond making and breaking (although the back reaction can be very slow). Secondly, the quantities  $a$  and  $K$  are strongly correlated with model functionality  $f$ , and since independent values are rarely available for any of these variables,  $f$  cannot usually be disentangled uniquely from  $a$  and  $K$ . More detail of such considerations is given in an extensive recent review<sup>12</sup> of biopolymer gels and gelation.

Fits to  $G'$  versus  $C$  data for the amylose DP = 300, 660, 1100, and 2550 gels (see earlier sections) were achieved by using the equation<sup>12,13,21</sup>

$$\frac{G'K(f-1)(f-2)}{aRT} = \frac{(f-1)^2\alpha(1-\nu)^2(1-\beta)}{2(f-2)} \frac{C}{C_0} \quad (1)$$

where  $\alpha$ ,  $\nu$ , and  $\beta$  are functions of  $f$  and  $C/C_0$  only. The functionality  $f$  was allowed to take on a series of values (e.g., 3, 5, 10, 20, 100, and 1000), and for each  $f$  the fitting procedure determined the corresponding best values for  $a$  and  $K$ .  $C_0$  was included in each case from the relationship<sup>12,13,21</sup>

$$C_0 = \frac{M(f-1)}{Kf(f-2)^2} \quad (2)$$

Tables I and II show the results obtained; in Table I the apparent front factor  $a$  decreases with  $f$ , whereas  $C_0$  is independent of  $f$ . Table II shows that, within experimental error,  $C_0$  is independent of the primary chain molecular weight, in direct contradiction with the assertion<sup>6</sup> that  $C_0$  should be equal to the chain overlap concentration  $C$  (see ref 22 for more details).

If we assume that the unknown functionality  $f$  should be equal to DP/110 (the chain length at which precipitation replaces gelation and therefore an estimate of the distance between the start of consecutive junction zones),  $a$  is, within the constraints of the model, found to be independent of DP for DP > 600. Similar results are also found for the constant  $K$ . Clearly, in view of all the uncertainties discussed so far it would be unwise to pursue a more detailed interpretation than has been attempted above. Suffice it to say that the modulus/concentration data made available for amylose gels in the present study

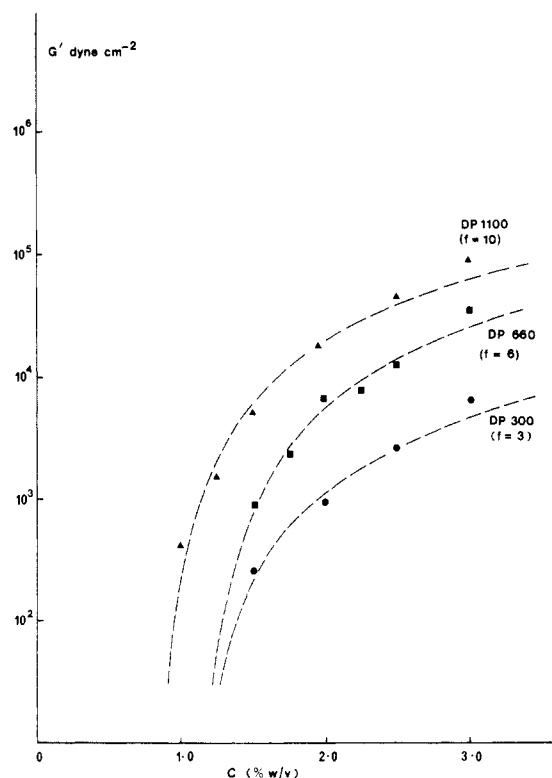


**Figure 5.** Experimental  $G'$  values vs concentration (% w/v) data for amylose gels: (●) DP = 300, (□) DP = 660, (▲) DP = 1100. Theoretical fits obtained by using the Clark-Ross-Murphy approach ( $f = 3, 6$ , and  $10$ ) are indicated by broken lines. For details see text.

can best be rationalized by assuming that  $f$  is roughly proportional to DP and that eq 1 describes the functional form of modulus-concentration curves. The actual fits achieved by the  $f = 3, 6$ , and  $10$  models to DP = 300, 660, and 1100 data appear in Figure 5.

In a recent paper,<sup>6</sup> Ellis and Ring charted the concentration dependence of gel modulus for pea amylose over the range 1.5–7.0% w/w and found that on average, over this range,  $G'$  (measured in a Ward and Saunders tube or a pulse shearometer) varied as  $C^7$  (not, as is more commonly reported for biopolymer gels,  $C^2$ ). On the basis of their data, they suggested that current theories for relating gel modulus to concentration were unlikely to be applicable.<sup>12,13,23</sup> The present analysis using one of these theories appears, therefore, to be in strict disagreement with their conclusions. However, if our experimental data (Figure 5) are replotted on a log-log scale, reasonably linear plots for each individual chain length are obtained, the slopes of which are 5.9 (DP = 1100), 4.7 (DP = 660), and 4.4 (DP = 300); i.e., slopes are obtained which are also considerably greater than 2. As Ellis and Ring<sup>6</sup> used an amylose sample of  $DP_w \sim 3000$ , their somewhat greater value of  $\sim 7$  is actually not inconsistent with the present data. This seeming paradox may be resolved if it is realized that apparently linear log  $G'$  vs log  $C$  plots and high power laws arise naturally out of the theoretical treatment used in the present study when low values (and restricted ranges) of the variable  $C/C_0$  are alone considered.<sup>12</sup> As can easily be verified from the theory,<sup>12,13</sup> however, these high (and  $C/C_0$  dependent) exponents eventually converge to a value close to 2 and become independent of  $C/C_0$  as  $C$  increases. Unfortunately, experimental verification of this fact for amylose gels is made particularly difficult (if not impossible) by the very rapid rigidification of samples at higher concentrations (even at quite elevated temperatures). For a biopolymer gel, however, it is only when this

terminal  $C/C_0$  regime has been accessed that a physically meaningful power law can be determined.

## Summary and Conclusions

From studies of aqueous solutions formed from essentially monodisperse amylose samples, the effects of chain length and concentration on gel properties (e.g., modulus and turbidity) have been studied. For each chain length (DP = 250–2800), increasing amylose concentration resulted in more rapid gelation/turbidity increase and higher pseudoequilibrium gel modulus values. Analysis of modulus/concentration data by the method of Clark and Ross-Murphy<sup>13</sup> showed the same general type of behavior previously found for other biopolymer gels<sup>12,13</sup> and predicted a critical gelling concentration of  $\sim 1.0\%$  w/v for all chain lengths as found by experiment.<sup>7</sup> Although the experimental modulus/concentration data could be fitted quantitatively by using a number of combinations of the parameters  $f$ ,  $K$ , and  $a$ , the reasonable assumption that  $f$  is proportional to chain length and that  $DP/f \sim 100$ , in accordance with experiment,<sup>7</sup> leads to the conclusion that values of  $a$  and  $K$  are nearly independent of chain length. This behavior would be expected if the same molecular mechanism is operative in amylose cross-linking (e.g., junction zone formation) irrespective of chain length.

As well as affecting modulus values, chain length also has a marked effect on the kinetics of amylose gelation, shorter chains leading to more rapid gelation and less subsequent annealing. For the longest chains studied (DP = 2500 and DP = 2800), gel annealing is so slow that pseudoequilibrium modulus values were not found in the initial 14 days. Turbidity increases were found to take place in all gelling systems with shorter chains exhibiting higher turbidity values at fixed times than gels formed from longer chains, suggesting that increasing chain length results in greater homogeneity of gel structure. Comparison of modulus and turbidity data during the formation of amylose gels showed that the relative rates of increase in the two properties are highly dependent on chain length. For short chains (DP = 250 and 300), turbidity increases precede modulus development, suggesting that some non-cross-linking aggregation (precipitation) occurs; for longer chains (DP > 1100), modulus increases occur before significant turbidity is apparent.

**Registry No.** Amylose, 9005-82-7.

## References and Notes

- (1) Banks, W.; Greenwood, C. T. *Starch and its Components*; Edinburgh University: Edinburgh, 1975.
- (2) Young, A. H. *Starch: Chemistry and Technology*, 2nd ed.; Academic: New York, 1984; pp 249–283.
- (3) Rutenburg, M. W. *Handbook of Water-Soluble Gums and Resins*; McGraw-Hill: New York, 1980; pp 22–1–22–83.
- (4) Miles, M. J.; Morris, V. J.; Orford, P. D.; Ring, S. G. *Carbohydr. Res.* **1985**, *135*, 271–281.
- (5) Miles, M. J.; Morris, V. J.; Ring, S. G. *Carbohydr. Res.* **1985**, *135*, 257–269.
- (6) Ellis, H. S.; Ring, S. G. *Carbohydr. Polym.* **1985**, *5*, 201–213.
- (7) Gidley, M. J.; Bulpin, P. V., first paper in a series in this issue.
- (8) Husemann, E.; Burchard, W.; Pfannmüller, B. *Stärke* **1964**, *16*, 143–150.
- (9) Pfannmüller, B.; Mayerhöfer, H.; Schultz, R. C. *Biopolymers* **1971**, *10*, 243–261.
- (10) Richardson, R. K.; Ross-Murphy, S. B. *Int. J. Biol. Macromol.* **1981**, *3*, 315–322.
- (11) Morris, E. R.; Ross-Murphy, S. B. *Tech. Life Sci. Biochem.* **1981**, *B310*, 1–46.
- (12) Clark, A. H.; Ross-Murphy, S. B. *Adv. Polym. Sci.* **1987**, *83*, 57–192.
- (13) Clark, A. H.; Ross-Murphy, S. B. *Br. Polym. J.* **1985**, *17*, 164–168.
- (14) Treloar, L. R. G. *The Physics of Rubber Elasticity*, 2nd ed.; Clarendon: Oxford, 1970.
- (15) Case, L. C. *J. Polym. Sci.* **1960**, *45*, 397–404.

- (16) Scanlan, J. J. *Polym. Sci.* **1960**, 43, 501-508.  
 (17) Richardson, R. K.; Ross-Murphy, S. B. *Int. J. Biol. Macromol.* **1981**, 3, 315-322.  
 (18) Clark, A. H.; Lee-Tuffnell, C. D. In *Functional Properties of Food Macromolecules*; Mitchell, J. R., Ledward, D. A., Eds.; Elsevier: Barking, U.K., 1986; pp 203-272.  
 (19) Lips, A.; Hart, P.; Clark, A. H. In *Gums & Stabilizers for the Food Industry-4*; Phillips, G. O., Wedlock, D. J., Williams, P. A., Eds.; IRL: Oxford, U.K., 1988, pp 39-50.  
 (20) Morris, E. R.; Rees, D. A.; Robinson, G. J. *Mol. Biol.* **1980**, 138, 349-362.  
 (21) Clark, A. H. In *Food Structure and Behavior*; Blanshard, J. M. V., Lillford, P., Eds.; Academic: London, 1987; Vol. 1, pp 29-50.  
 (22) Gidley, M. J., third paper in a series in this issue.  
 (23) Oakenfull, D. G. *J. Food Sci.* **1984**, 49, 1103-1110.

## Molecular Mechanisms Underlying Amylose Aggregation and Gelation

Michael J. Gidley

Unilever Research Laboratory, Colworth House, Sharnbrook, Bedford, MK44 1LQ, U.K.  
 Received January 20, 1988; Revised Manuscript Received June 2, 1988

**ABSTRACT:** The molecular origin of the aqueous aggregation and gelation behavior of amylose is shown to lie in the formation of interchain double helices. Gelation is shown to be possible from "dilute" nonentangled amylose solutions, and no correlation is found between critical gelling concentrations and coil overlap concentrations for a range of amylose chain lengths. NMR and X-ray diffraction experiments show that amyloses precipitated from dilute aqueous solution contain only B-type aggregated double helices and that amylose gels contain rigid double-helical "junction zones" interconnected by more mobile amorphous single-chain segments. Optical rotation results suggest that the double-helix structure underlying amylose aggregation and gelation may have a left-handed conformation.

### Introduction

In the previous two papers in this issue,<sup>1,2</sup> the aggregation and gelation behavior of enzymically synthesized and nearly monodisperse amylose samples has been described. These studies showed that polymer chain length has a profound effect on the aggregation processes that take place from (inherently unstable) aqueous amylose solutions. Thus the physical form (i.e., precipitate, gel, etc.), the kinetics of aggregation as monitored by turbidimetry<sup>1,2</sup> and rheology,<sup>2</sup> and the variation of gel strength with concentration<sup>2</sup> all show a dependence on the amylose chain length. The effects observed were rationalized on the basis of polymer-polymer cross-linking occurring over limited (typically less than 100 residues) regions of amylose chains.<sup>1,2</sup>

It is well established that amylose in aqueous solution has the hydrodynamic properties of a random coil.<sup>3,4</sup> Furthermore, it has been known for a long time that aged amylose gels show partial crystallinity<sup>5</sup> (as judged by X-ray diffraction). The diffraction pattern obtained from aqueous gels and precipitates is of the B type, characteristic of root, tuber, and stem granular starches.<sup>6,7</sup> It has recently been shown that B-type diffraction patterns are due to an ordered array of hexagonally packed double helices.<sup>7</sup> Although the helix packing arrangement in B-type crystallites appears to be well established, other structural details such as helix handedness<sup>8</sup> and packing sense<sup>9</sup> have still to be determined unambiguously.

From the above discussion, it can be seen that amylose aggregation/gelation eventually results in the conversion of at least some random coils into highly ordered crystalline structures. The molecular mechanisms involved in this conversion are the subject of current debate. Thus, Miles et al. have suggested<sup>10</sup> that gels are formed upon cooling molecularly entangled solutions as a result of phase separation, with subsequent crystallization occurring in the polymer-rich phase, whereas Sarko and Wu have proposed<sup>11</sup> that gelation occurs because of chain cross-linking by double-helical junction zones. The aim of our study was to examine the concentration regimes from which gelation occurs for amylose and to probe the molecular

structures present and the transformations that occur during aqueous amylose aggregation.

### Experimental Section

All amyloses were either synthesized enzymatically<sup>1</sup> or obtained commercially (potato amylose, Sigma), and solutions were prepared as described previously.<sup>1,2</sup>

Viscosity measurements were carried out at 303 K on a Contraves Low Shear 30 viscometer (Couette geometry—maximum shear rate 1 s<sup>-1</sup>), extrapolated to "zero-shear" conditions,<sup>12</sup> and repeated 2-3 times for 2-3 replicates of the sample solution. For some aqueous amylose systems, viscosity values were found to increase markedly with time (1-5 min), suggesting the onset of polymer aggregation although visible signs of aggregation (e.g., turbidity, microgel formation) were not apparent. For characterization of the coil overlap concentration, aggregation effects need to be avoided, and therefore viscosity values were considered to be reliable only if essentially identical results were obtained following at least one repeat measurement on the same sample 1-2 min after the initial experiment.

X-ray diffraction measurements were made by using a Phillips powder diffractometer (PCW 1050/1390) mounted on a PW 1730/10 sealed tube X-ray generator operating at the Cu K $\alpha$  wavelength (1.542 Å).

<sup>13</sup>C NMR spectra were obtained on a Bruker CXP-300 instrument operating at 75.46 MHz, and spectra were referenced to external Me<sub>4</sub>Si via the low-field resonance of solid adamantane (38.6 ppm). All <sup>13</sup>C spectra were obtained by using cylindrical sample holders in a double-bearing "solid" probe head (DB/MAS). For cross polarization and magic angle spinning spectra, spinning rates of 3-4 KHz and spin locking and <sup>1</sup>H decoupling fields of ~80 kHz (20 gauss) were employed. Other experimental parameters were as follows: acquisition time, 140 ms; recycle delay, 4 s; time domain points, 8 K, and transform size, 32 K. For <sup>1</sup>H NMR analysis, amylose samples were dissolved in D<sub>2</sub>O (433 K, 15 min), lyophilized, and redissolved in D<sub>2</sub>O. High-resolution <sup>1</sup>H NMR spectra were obtained on a Bruker AM200 instrument operating at 200.13 MHz. A 10-s delay between successive 90° pulses was employed to ensure complete relaxation. The variation of amylose signal area as a function of time and temperature was determined by comparison with the signal area due to a pyrazine standard in a coaxial tube. <sup>1</sup>H NMR T<sub>2</sub> values were determined by direct measurement of the free induction decay immediately following the initial 90° pulse in a Carr-Purcell-Meiboom-Gill (CPMG) pulse sequence as well as from the amplitudes of sub-